NASA Technical Memorandum 106833

Enhanced Capabilities and Modified Users Manual for Axial-Flow Compressor Conceptual Design Code CSPAN

Arthur J. Glassman
University of Toledo
Toledo, Ohio

and

Thomas M. Lavelle
Lewis Research Center
Cleveland, Ohio

January 1995

National Aeronautics and Space Administration

Enhanced Capabilities and Modified Users Manual for Axial-Flow Compressor Conceptual Design Code CSPAN

Arthur J. Glassman*
University of Toledo
Toledo, Ohio 43606
and
Thomas M. Lavelle
National Aeronautics and Space Administration
Lewis Research Center
Cleveland, Ohio 44135

SUMMARY

This report presents modifications made to the computer code CSPAN, which is a conceptual sizing analysis for axial-flow compressors. The CSPAN analysis uses a rapid approximate design methodology based on isentropic simple radial equilibrium to determine the flowpath either for a given number of stages or for a given overall pressure ratio. Calculations are performed at constant span-fraction locations from tip to hub. Stage energy addition is controlled by specifying the maximum allowable values for several aerodynamic design parameters.

Modifications were made to CSPAN to enhance code capabilities, upgrade loss modeling, and improve user convenience. Added to the code were endwall blockage and stall margin predictions. Endwall blockage is calculated using an annulus boundary-layer model. Stall margin is estimated by diffuser analogy. The pressure-loss coefficient model, which had been based on cascade data, was replaced by one that had been successfully tested against several multistage compressors.

Default correlations for rotor and stator solidities and aspect ratios and for stator-exit tangential velocity along with default values for the aerodynamic design limits have been added to the code as an aid for non-expert users in selecting reasonable values for these inputs. The solidity and aspect ratio correlations were based on values used for the design of five transonic core compressors. Aerodynamic design limits for rotor and stator diffusions, rotor hub turning, and stator-hub Mach number were based on design experience.

This report also serves as an updated users manual for the modified CSPAN code. Program input and output are described, and sample cases are included for illustration.

INTRODUCTION

Performing engine studies requires the capability to rapidly produce conceptual designs of the components in order to determine geometry, performance, and weight. The typical compressor "design" code enables a study of the interrelationship of the number of stages, the flowpath radii, the gas velocities, the flow angles, and the resultant variation of compressor efficiency. A computer code capable of performing this function in a rapid approximate manner was presented in reference 1. An updated version of this code (named CSPAN) with

*Resident Research Associate at NASA Lewis Research Center.

numerous modeling improvements was presented in reference 2, and subsequent blade geometry modeling added to the code was reported in reference 3.

Additional capabilities were recently added to CSPAN. Presented in reference 4 are a method for the calculation of endwall blockage as well as correlations for determining the losses at minimum-loss incidence. Correlations for the calculation of maximum loading capability for a compressor are presented in reference 5. These methods, all based on meanline parameters and thus consistent with a rapid calculation procedure, were added to CSPAN. In addition, it became evident that non-expert users needed guidance in the specification of inputs. Therefore, default correlations were added for rotor and stator solidities and aspect ratios and for stator-exit tangential velocities, and upper limits were included as defaults for the input parameters reflecting aerodynamic design severity.

This report presents the analytical modeling associated with the new capabilities added to the CSPAN code. It also serves as an updated users manual for the code. Program input and output are described and sample cases are included for illustration.

SYMBOLS

A	area, ft^2
$\mathcal{A}$	aspect ratio
B	coefficient in tangential velocity equation (eq.(16)), (ft)(in.)/sec
C	coefficient in tangential velocity equation (eq.(16)), ft/sec
C_f	friction coefficient
c	chord, ft
D	diffusion factor
$\mathbf{D}_{eq}$	equivalent diffusion ratio
D	coefficient in tangential velocity equation (eq.(16)), ft/(sec)(in.)
E	coefficient in tangential velocity equation (eq.(16)), ft/(sec)($in.^2$)
F	axial blade-force defect, lbm/sec^2
g	gravitational constant, 32.17 (lbm)(ft)/(lbf)(sec^2)
H	form factor
h	blade height, ft
Δh	stage specific work, Btu/lbm
i	stage number
J	conversion constant, (ft)(lbf)/Btu
L_i	ideal pressure-rise coefficient
M	Mach number
n	number of stages
PR	pressure ratio
p	pressure, psi
R	reaction
r	radius, in.

U	blade speed, ft/sec
V	relative (for rotors) or absolute (for stators) velocity, ft/sec
β	relative (for rotors) or absolute (for stators) flow angle from axial direction, deg
δ	displacement thickness, ft
θ	momentum thickness, ft
ρ	density, lb/ft^3
σ	solidity
ϕ_{eq}	equivalent divergence angle, deg
ω	pressure loss coefficient

Subscripts:

ew	endwall
h	hub
i	stage number index
lf	lift forces
m	mean
max	maximum
mid	middle
p	profile
r	rotor
rel	relative
s	stator
sf	streamwise forces
sh	shock
st	stall
t	tip
tot	total
u	absolute tangential component
x	axial component
0	stagnation
1	rotor inlet or cascade inlet
2	rotor exit / stator inlet or cascade exit
3	stator exit

Superscript:

*	at peak efficiency

ANALYTICAL MODELING

The analytical models for the new/modified capabilities added to CSPAN are discussed in this section. These features are endwall blockage, stall margin, loss coefficients, and input defaults. Where the detailed methodologies can be referenced, only the key assumptions

and equations are presented here.

Endwall Blockage

The endwall blockage calculation uses the methodology of Wright and Miller (ref. 4), which is an application of the formulation of De Ruyck and Hirsch (ref. 6). This method is based on a 2D incompressible semi-empirical model for the growth of endwall boundary-layer momentum thickness across a blade row:

$$\theta_2 - \theta_1 = c_x C_f/(2\cos\beta_m) - \theta_m(2+H_m)(V_{x,2}-V_{x,1})/V_{x,m} + F_{x,sf}/(\rho V_{x,m}^2) + F_{x,lf}/(\rho V_{x,m}^2) \qquad (1)$$

The first two terms on the right hand side of this equation are the skin friction and the axial-velocity ratio effects. The last two terms account for changes in the axial component of blade force through the endwall boundary layer due to dissipation forces along the streamlines and lift forces at right angles to the streamlines.

The empirical expressions required to evaluate the blade-force terms of equation (1) are presented in reference 4. To complete the system of equations, Greens entrainment equation (presented in ref. 4) for a simple power-law velocity profile is used.

$$V_{x,2}\theta_2 H_2/(H_2-1) - V_{x,1}\theta_1 H_1/(H_1-1) = 0.0153 c_x V_{x,m}[2H_m/(H_m-1)-3]^{-0.653} \qquad (2)$$

Once the exit momentum thickness and the exit form factor are solved for, the exit displacement thickness is found as

$$\delta_2 = H_2\,\theta_2 \qquad (3)$$

The tip and hub blockage factor inputs are then calculated as

$$DTIP = 1 - \delta_t(2r_t-\delta_t)/(r_t^2-r_h^2) \qquad (4a)$$

and

$$DH = 1 - \delta_h(2r_h+\delta_h)/(r_t^2-r_h^2) \qquad (4b)$$

where (1-DTIP) and (1-DH) are the endwall-area blockages at the tip and hub, respectively.

The total endwall-area blockage (tip plus hub) calculated at stage exit for the five core compressors used as the performance database in reference 2 are plotted against stage number in figure 1. Unfortunately, there seems to be no readily available data against which to compare the predictions. The calculated values are reasonably consistent with general experience. The large blockage for the three-stage compressor reflects a very highly loaded design with turning of the flow back to axial direction in all stators. The large increase

(dashed line) in the last stage of one of the ten-stage compressors results from modeling limitations in CSPAN wherein one stator row is used to model two exit-stator rows in the actual compressor. If desired, this calculation can be bypassed in favor of using default or input blockages.

Stall Margin

A maximum loading prediction system for determining the design-speed stall margin of axial compressors was reported by Schweitzer and Garberoglio (ref. 5). The primary correlations are based on the analogy between a compressor cascade and a diffuser passage. Semi-empirical correlations are used to relate the cascade-derived maximum loading values to the real compressor environment.

Diffuser performance has been shown to depend on geometric parameters reflecting the amount of diffusion, as can be expressed by area ratio, and the rate of diffusion, as can be expressed by divergence angle. For incompressible flow, the area ratio alone sets the ideal loading

$$L_i = \Delta p/(p_{0,1}-p_1) = 1 - (A_1/A_2)^2 \qquad (5)$$

which for a two-dimensional compressor cascade can be expressed

$$L_i = 1 - (\cos \beta_1/\cos \beta_2)^2 \qquad (6)$$

An equivalent divergence angle for the same cascade can be expressed

$$\tan \phi_{eq} = [\mathcal{A}/(\pi\sigma)]^{1/2}(\cos^{1/2}\beta_2 - \cos^{1/2}\beta_1) \qquad (7)$$

Since any given area ratio for a compressor cascade can be attained by different combinations of inlet and exit angles as stagger is varied, blade row turning (β_1-β_2) was included as an additional correlation parameter.

With the above three parameters as independent variables, cascade data were used to develop a correlation for determining maximum static pressure-rise coefficient

$$[\Delta p/(p_{0,1}-p_1)]_{max} = f(L_i^*,\phi_{eq},\Delta\beta) \qquad (8)$$

Corrections for several flow and geometry parameters (e.g., Reynolds number, endwall boundary-layer thickness, tip clearance, etc.) affecting pressure-rise capability must be made to obtain the individual blade-row coefficients. The maximum pressure-rise coefficient for each blade row is then used to calculate a relative loading parameter (ratio of actual to maximum pressure-rise coefficient) which is then averaged into a stall indicator for the whole compressor. Finally, a linear correlation of stall margin versus stall indicator, determined from data for numerous compressors, is used to predict the peak-efficiency stall margin. The

correlations and corrections are presented in detail in reference 5.

The stall margin predicted by this method is a constant-flow stall margin

$$SM = (PR_{st} - PR^{*}) / PR_{st} \times 100 \qquad (9)$$

Table 1 presents a comparison between the stall margin predicted by CSPAN using these correlations and experimentally demonstrated values for the five core compressors and one fan used as the reference 2 database. It should be noted that there is a significant degree of uncertainty associated with the experimental values because (1) the compressors are not fully developed and (2) the near-vertical design-speed lines and the data scatter make it difficult to determine accurately the pressure ratio at peak efficiency. In fact, the pressure ratio at peak efficiency could not even be estimated for the five-stage compressor. The comparison, however, does indicate that this prediction calculation can be used as a qualitative measure of stall-margin adequacy.

Loss Coefficients

The existing cascade-based pressure-loss coefficient model (ref. 2) was replaced by a meanline model (ref. 4) that was developed and validated using compressor test results. This new model, which accounts for several dependencies (e.g., Mach no., Reynolds no., tip clearance, etc.) not found in the previous model, includes profile loss, endwall loss, and shock loss components.

The profile loss model has its basis in the same classical two-dimensional low-speed correlation method as previously used, but with modifications to account for compressibility and blade-thickness effects. Thickness-to-chord ratio was included by correlation into the definition of equivalent diffusion ratio (ratio of surface maximum velocity to inlet velocity). A second correlation then relates the classical loss parameter to the equivalent diffusion ratio and inlet Mach number.

$$\theta_p / c = \omega_p \cos \beta_2 (V_1^2/V_2^2)/(2\sigma) = f(\mathbf{D}_{eq}, M_1) \qquad (10)$$

Endwall loss effects have been treated in a similar manner by using the conservation of axial momentum to relate endwall boundary-layer momentum thickness to total-pressure loss. Based on experimental observations, the endwall loss parameter depended on tip clearance and loading, and a correlation of the form

$$2\,\theta_{ew} / c = \omega_{ew}(h/c)(V_1^2/V_2^2) = f(\mathbf{D}, \varepsilon/c) \qquad (11)$$

was used. Both the profile and the endwall loss coefficients are corrected for Reynolds number.

The shock loss calculation methodology is the same as was used in reference 2 except

for the correction to the normal shock loss, which in reference 4 was taken as 0.65 of the normal shock loss rather than as the normal shock loss divided by the square of the average Mach number as used in reference 2. However, the shock loss calculation in reference 4 was extended into the region of subsonic inlet Mach number. A shock loss is taken if the peak Mach number on the suction surface exceeds 1.08. All correlations and methods necessary to determine the total blade-row pressure-loss coefficients

$$\omega_{tot} = \omega_p + \omega_{ew} + \omega_{sh} \qquad (12)$$

are given in reference 4.

Efficiencies were calculated with this loss model and compared to efficiencies determined from experimental data for the five core compressors and one fan used as database in reference 2. As discussed therein, the experimental values presented for the design-point efficiencies were in some cases adjusted to account for the undeveloped state of these machines. Initial comparison of calculated and experimental efficiencies resulted in the use of a calibration coefficient to increase the profile and endwall losses by ten percent. This calibration amounts to about one point in efficiency. The comparison between calculated (after calibration) and experimental efficiencies is presented in table I. All calculated efficiencies match the experimental values to within one point, which is quite good.

Input Defaults

There are several geometric and aerodynamic inputs for CSPAN that require some user experience in compressor design/analysis to provide "reasonable" values. These include rotor and stator solidities and aspect ratios, stator-exit tangential velocities, and limiting values for rotor-tip and stator-hub diffusion factors, rotor-hub turning, and stator-inlet-hub Mach number. Default correlations/values based on the database compressors have been provided for these parameters and are presented in this section.

Solidity.- Within each of the compressors, there was a strong correlation between rotor-tip solidity and rotor-tip-inlet relative Mach number. The following linear equation was found to yield solidities generally within 10 percent of the actual solidities for all the stages of the database compressors.

$$\sigma_{r,t} = 0.5\, M_{t,1,rel} + 0.7 \qquad (13)$$

This equation should give reasonable estimates over the range of Mach numbers normally encountered in subsonic and transonic designs.

Stator-hub solidity showed a correlation with stator-hub turning, which is a measure of flow diffusion. Very limited data above 45 degrees of turning hints at an increased slope in this region, as is reflected in the following default correlation:

$\Delta\beta_{s,h}<44$ deg: $$\sigma_{s,h} = 0.0206\Delta\beta_{s,h} + 0.794 \quad (14a)$$

$44<\Delta\beta_{s,h}<60$ deg: $$\sigma_{s,h} = 0.080\Delta\beta_{s,h} - 1.82 \quad (14b)$$

$\Delta\beta_{s,h}>60$ deg: $$\sigma_{s,h} = 3.0 \quad (14c)$$

The stator-hub solidity is limited to a maximum value of 3, which corresponds to a turning of 60 degrees (well above conventional design practice).

Aspect ratio.- Aspect ratio depends primarily on stage location and also on design practice (i.e., conventional versus low aspect ratio) for high loadings. A linear variation from inlet to exit was adopted. Default conventional aspect ratios for both rotors and stators were based on a value of 2.5 for the first stage and 1.0 for the last stage. Thus,

$$\mathcal{A} = 1.5(n - i)/(n - 1) + 1.0 \quad (15a)$$

for conventional aspect-ratio blading. Low aspect-ratio blading is based on 1.5 for the first stage and 1.0 for the last stage; thus,

$$\mathcal{A} = 0.5(n - i)/(n - 1) + 1.0 \quad (15b)$$

Stator-exit tangential velocity.- The value of stator-exit tangential velocity and its variation with radius is specified for each stator by

$$V_{u,3} = B/r + C + Dr + Er^2 \quad (16)$$

where B, C, D, and E are inputs. Setting C=D=E=0.0 yields a free-vortex distribution of tangential velocity, which should suffice for conceptual design studies.

The tangential velocity of the flow leaving a stator is equal to that entering the following rotor and, thus, defines the reaction of that following stage. Combining the definition of reaction (eqn. (2-39) of ref. 7), the Euler work equation (eqn. (2-14) of ref. 7), and the tangential-component vector relationship (eqn. (2-6) of ref. 7) and assuming constant blade speed and axial velocity across the stage along with equal stage work yields an equation for stator-exit tangential velocity as a function of the reaction of the next stage:

$$V_{u,3,i-1} = (1-R_i)U_i - gJ\Sigma\Delta h_i/(2nU_i) \quad (17)$$

Applying equation (17) to the tip section, where blade speeds are known from input, assuming a polytropic efficiency of 0.9 to estimate overall specific work from the input pressure ratio, and specifying reaction, either from an input or default parameter, allows the stator-exit tangential velocity for the previous stage to be estimated. With the assumption of free-vortex flow in equation (16), the input variable defining stator-exit tangential velocity can then be found from:

$$B3(i) = r_{t,3,i}V_{u,t,3,i} \quad (18)$$

A methodology to determine the stage-exit tangential velocity for all the stages was adopted wherein reaction would decrease from the first stage to a mid stage and then increase from there to the last stage. For the first stage, the rotor-inlet tangential velocity, for free-vortex flow, is defined by the input variable B1. A value for B1 can be input directly or, as newly added to the program, determined from an input or default (10 deg.) value for first-stage-rotor tip inlet absolute angle.

$$B1 = r_{t,1,1}V_{u,t,1,1} = r_{t,1,1}V_{x,t,1,1}\tan \beta_{t,1,1} \quad (19)$$

The axial velocity is determined by continuity.

The mid stage, for which a tip reaction is specified by input or default (0.6), is defined for an even number of stages as

$$i_{mid} = n/2 + 1 \quad (20a)$$

and for an odd number of stages as

$$i_{mid} = (n+1)/2 \quad (20b)$$

The value of $B3(i_{mid}-1)$ is then determined from equations (17) and (18) using the specified tip reaction. Because of the assumptions associated with equation (17), the reaction for stage i_{mid} will only approximate the specified value.

Finally, B3(n-1) is taken as half of $B3(i_{mid}-1)$, and B3(n) is set to zero. The B3 values for the remaining stages are found by linear interpolation between B1 and $B3(i_{mid}-1)$ for the front half of the compressor and linear interpolation between $B3(i_{mid}-1)$ and B3(n-1) for the rear of the compressor. This default distribution for B3 is used only in the absence of input values.

Aerodynamic design limits.- The design calculation is executed with maximum allowable values for rotor-tip and stator-hub diffusion factors, rotor-hub turning, and stator-inlet-hub Mach number for each stage. Default values assigned to these design limits are:

rotor-tip diffusion factor: 0.5
stator-hub diffusion factor: 0.6
rotor-hub turning: 40 deg.
stator-inlet-hub Mach number: 0.85

These values, which may be overridden by input, reflect current technology limits for good performance.

DESCRIPTION OF INPUT AND OUTPUT

This section presents a complete description of the input and the output for the updated CSPAN program. Included with the input and output are sample cases for a five-stage transonic compressor.

Input

The input, which is read on unit 05, consists of a title line and one NAMELIST dataset. Input for the sample case is presented in table II. The title, which is printed as a heading on the output file, can contain up to 71 characters located anywhere in columns 2 through 72 on the title line. A title, even if it is left blank, must be the first record of the input data.

The physical data and option switches are input in data sets having the NAMELIST name NAME. The variables that compose NAME are defined herein along with units and default values. They are presented in order as general inputs, inlet inputs, rotor inputs, and stator inputs.

General:

MW — molecular weight of working fluid, lb/(lb mol) (default=28.97)

GAM — specific heat ratio (default=1.4)

RCLIM — limit value for overall pressure ratio

NSLIM — limit value for number of stages

N — number of calculation locations from tip to hub

ICV — pressure ratio convergence switch (default=1)

- 0 - accepts overall pressure ratio equal to or greater than RCLIM as a solution
- 1 - converges to overall pressure ratio RCLIM

IPR1 — debug output switch (default=0)

- 0 - no debug output
- 1 - minimum debug output
- 2 - extensive debug output

IPR2 — radial location output switch (default=0)

- 0 - output printed for all radial calculation locations
- 1 - output printed for tip and hub only

WK	loss multiplier, increases total loss for polytropic efficiency correlation and profile/endwall losses for pressure-loss coefficient correlation (default=1.0)
IIT	technology-level indicator for polytropic efficiency (default=1) 1 - current technology, equations (8) and (9) of ref. 2 2 - advanced technology, equations (10) and (11) of ref. 2
IPATH	flowpath slope switch (default=0) 0 - flowpath slope is average of previous and next blade-row slopes 1 - flowpath slope equals zero
CSTAL	stall margin coefficient, larger value reduces stall margin (default=1.0)
VIS	gas viscosity, lbm/(sec)(ft) (default=-1.) <0.0 - internal computation of viscosity for air >0.0 - value of viscosity
IBLOCK	endwall blockage calculation switch (default=0) 0 - blockage is calculated 1 - default or input blockages are used
Inlet:	
TTI	inlet total temperature, °R
PTI	inlet total pressure, psi
RTIP1I	tip radius at first-rotor inlet, in.
UTIP1I	blade speed at first-rotor inlet tip, ft/sec
RHORT1	hub/tip radius ratio at first-rotor inlet
VZTIPO	inlet axial velocity or mass flow >0 - VZTIPO is the axial velocity at the first-rotor inlet tip, ft/sec <0 - |VZTIPO| is the mass flow rate, lb/sec
DTIP1	tip blockage factor at first rotor inlet (default=0.99)
DH1	hub blockage factor at first-rotor inlet (default=0.99)

DPPIGV inlet guide vane total-pressure loss fraction (default=0.0 if B1 is input, default=0.005 if B1 is omitted and BETA1T>0.0 and DPPIGV=0.0 or omitted)

BETA1T absolute flow angle at first-rotor inlet tip; BETA1T is used only if B1 is omitted, deg (default=10.0)

B1 coefficient B for equation (16) at first-rotor inlet, omit to use BETA1T to define B1 per equation (19), (ft)(in.)/sec

C1 coefficient C for equation (16) at first-rotor inlet, ft/sec (default=0.0)

D1 coefficient D for equation (16) at first-rotor inlet, ft/(sec)(in.) (default=0.0)

E1 coefficient E for equation (16) at first-rotor inlet, ft/(sec)(in.^{2}) (default=0.0)

Rotor: Each subscripted variable requires NSLIM values.

RT2OT1(I) ratio of exit-tip radius to inlet-tip radius for each rotor (default=NSLIM * 1.0)

VT2OT1(I) ratio of exit-tip meridional velocity to inlet-tip meridional velocity for each rotor (default=NSLIM * 1.0)

NPRI(I) efficiency specifier for each rotor
> 0.0 - input value is rotor polytropic efficiency
= 0.0 - polytropic efficiency correlation is used
=-1.0 - pressure-loss coefficient correlation is used

SRTIP(I) rotor-tip solidity (default=-1.)
> 0.0 - input value is rotor tip solidity
=-1.0 - default correlation (eqn. (13)) is used

ARO(I) rotor aspect ratio, based on actual chord (default=-1.)
> 0.0 - input value is rotor aspect ratio
=-1.0 - conventional aspect-ratio correlation (eqn. (15a)) is used
=-2.0 - low aspect-ratio correlation (eqn. (15b)) is used

DTIP2(I) tip blockage factor at rotor exit (default=.99,.985,.98,.975,.97,.965,.96,.955,.95 ... .95)

DH2(I) hub blockage factor at rotor exit (default=.99,.985,.98,.975,.97,.965,.96,.955,.95 ... .95)

ARHD(I) rotor-hub ramp angle limit, deg (default=NSLIM * 40.0)

ARTD(I) rotor-tip ramp angle limit, deg (default=NSLIM * -20.0)

DRT(I) rotor-tip diffusion factor maximum allowable value (default=NSLIM * 0.5)
> 0.0 - DRT is used to compute coefficient B (eqn. (16)) at rotor exit
= 0.0 - BO is used as coefficient B (eqn. (16)) at rotor exit

BO(I) coefficient B for equation (16) at rotor exit, required only if DRT(I)=0.0, (ft)(in.)/sec

C2(I) coefficient C for equation (16) at rotor exit, ft/sec (default=NSLIM * 0.0)

D2(I) coefficient D for equation (16) at rotor exit, ft/(sec)(in.) (default=NSLIM * 0.0)

E2(I) coefficient E for equation (16) at rotor exit, ft/(sec)(in.^{2}) (default=NSLIM * 0.0)

BPSD(I) maximum allowable value for rotor-hub turning, deg (default=NSLIM * 40.)

TCR rotor maximum thickness to chord ratio (default=0.06)

EHR rotor tip-clearance to blade-height ratio (default=0.01)

Stator: Each subscripted variable requires NSLIM values.

RT3OT2(I) ratio of exit-tip radius to inlet-tip radius for each stator (default=NSLIM * 1.0)

VT3OT2(I) ratio of exit-tip meridional velocity to inlet-tip meridional velocity for each stator (default=NSLIM * 1.0)

NPSI(I) efficiency specifier for each stage
> 0.0 - input value is stage polytropic efficiency
= 0.0 - polytropic efficiency correlation is used
=-1.0 - pressure-loss coefficient correlation is used for stator

SSH(I) stator-hub solidity (default=-1.)
> 0.0 - input value is stator hub solidity
=-1.0 - default correlation (eqns. (14)) are used

ASO(I) stator aspect ratio, based on actual chord (default=-1.0)
> 0.0 - input value is stotor-hub solidity
=-1.0 - conventional aspect-ratio correlation (eqn. (15a)) is used
=-2.0 - low aspect-ratio correlation (eqn. (15b)) is used

DTIP3(I)	tip blockage factor at stator exit (default=.985,.98,.975,.97,.965,.96,.955,.95 ... .95)
DH3(I)	hub blockage factor at stator exit (default=.985,.98,.975,.97,.965,.96,.955,.95 ... .95)
ASHD(I)	stator-hub ramp angle limit, deg (default=NSLIM * 40.0)
ASTD(I)	stator-tip ramp angle limit, deg (default=NSLIM * -20.0)
DSH(I)	maximum allowable value for stator-hub diffusion factor (default=NSLIM * 0.6)
MSH(I)	maximum allowable value for stator-inlet-hub Mach no. (default=NSLIM * 0.85)
B3(I)	coefficient B for equation (16) at stator exit, omit to use a default B3 distribution based on mid-stage reaction (REACT), (ft)(in.)/sec
C3(I)	coefficient C for equation (16) at stator exit, ft/sec (default=NSLIM * 0.0)
D3(I)	coefficient D for equation (16) at stator exit, ft/(sec)(in.) (default=NSLIM * 0.0)
E3(I)	coefficient E for equation (16) at stator exit, ft/(sec)(in.^{2}) (default=NSLIM * 0.0)
REACT	tip reaction used to compute B3 for the middle stage (eqns. (17) and (18)), REACT is used only if B3(1) is omitted (default=0.6)
TCS	stator maximum thickness to chord ratio (default=0.06)
EHS	stator tip-clearance to blade-height ratio (default=0.0)

The sample input file shown in table II contains two cases for a five-stage transonic compressor. Each case begins with a title card. The first case makes use of all the default values and, thus, requires a minimum of additional input. The second case uses input values consistent with those for the actual compressor.

Output

Program output consists of a main output file written to unit 06 and, where convergence to the given overall pressure ratio is specified, a brief convergence file written to unit 08, which is directed to the terminal. The main output presents either the results of a completed design calculation or an error message indicating the nature of the failure.

Outputs corresponding to the sample input of table II are presented in tables III and IV. The pressure-ratio convergence output, shown in table III, is sent to the terminal so that a convergence problem or a failure to meet design requirements can be immediately detected.

Convergence problems are rare, but unsatisfactory or unexpected design solutions can occur in any preliminary study. As seen from table III, the first case could not produce the desired compressor pressure ratio (CPR) of 5 in five stages within the prescribed constraints. A pressure ratio of only 4.74 was obtained due to the stator-inlet-hub Mach number limit constraining the stage energy addition in the first four stages.

For the second case, it can be seen from table III that convergence to a compressor pressure ratio of 5 was achieved in four iterations. Shown in the output are the number of stages followed by one line for each iteration displaying the rotor-tip diffusion reduction factor (DRTK), the compressor pressure ratio (CPR), and the compressor adiabatic efficiency (EFF). The velocity diagram specified for this case had a reduced stator-inlet Mach number and, thus, enabled an increase in stage energy addition without exceeding the prescribed stator Mach number limit.

The main output is presented in table IV. For brevity in displaying the output, calculations were performed at only three radial locations (N=3), and only stages 1 and 5 of the second case are included along with the overall and inlet information. The first line of output in table IV is the title; it is followed by identification of the loss model used for this case. Then, the general inputs and the inlet inputs are printed. The values displayed are clearly identified.

The next output line in table IV states that one of the aerodynamic limits, in this case the stator hub Mach number, was exceeded in the next stage, which in this case is the first stage. As a result, the rotor-tip diffusion factor was reduced from its maximum allowable value until the Mach number limit was just satisfied. The consequence of this, as indicated above, is a reduction in stage pressure ratio.

The next block of output in table IV is the data for stage 1. This includes the rotor input, the stator input, the cumulative and stage performance, the stage flowpath geometry, the detailed aerodynamic results at the rotor inlet, the rotor exit, and the stator exit, and finally the blading geometry. Note that the rotor and stator input sections include the rotor and stage polytropic efficiencies, respectively, which were determined in this case from the internal loss-coefficient correlation. These input sections also include solidities, aspect ratios, and blockage factors, all of which may be either input or determined internally from correlations.

Under stage output data are the overall (i.e., cumulative) values of pressure ratio, temperature ratio, and adiabatic efficiency followed by the stage values, which are here the same since this is the first stage. Also displayed under this heading are the rotor and stator tip and hub radii, the axial lengths, and the tip and hub ramp angles. At each of the three axial stations for the stage (i.e., rotor inlet, rotor exit, and stator exit) are presented among other parameters, the temperatures and pressures, the absolute and relative velocities, the absolute and relative flow angles, the diffusion factors, and the loss coefficients at each of the radial calculation locations.

Finally, the rotor and stator blading geometries are presented for each of the radial sections. Included are numbers of blades, chord lengths, aspect ratios, solidities, camber angles, incidence and deviation angles, and blading angles.

The stage data format is identical for each stage; therefore, the "STAGE DATA" output for stages 2, 3, and 4 were omitted from table IV. Shown next is the data for stage 5. The "STAGE OUTPUT DATA" show that the overall pressure ratio of 5 has been achieved with an overall efficiency of 0.867. For this constant-tip-radius (10 in.) design, the hub radius increased from 5.0 in. at the first-rotor inlet to 8.33 in. at the last-stator exit. For the last stage, the computed stall margin is displayed after the blading geometry data. The last line of output states that the specified overall pressure ratio has been achieved. If the specified pressure ratio had not been achieved, the last-line message would be that the maximum number of stages had been reached.

SUMMARY OF RESULTS

This report presents modifications made to the computer code CSPAN, which is a conceptual sizing analysis for axial-flow compressors. The CSPAN analysis uses a rapid approximate design methodology based on isentropic simple radial equilibrium to determine the flowpath either for a given number of stages or for a given overall pressure ratio. Calculations are performed at constant span-fraction locations from tip to hub. Stage energy addition is controlled by specifying the maximum allowable values for several aerodynamic parameters.

Modifications made to CSPAN and reported herein resulted in additional capabilities, improved modeling, and user convenience. Specifically:

1. An endwall blockage calculation was added. This was based on a semi-empirical model for the growth of endwall boundary-layer momentum thickness across a blade row. Predictions for five core compressors yield results that appear to be reasonable, but there is no readily available data against which to compare the computed results.

2. Stall margin prediction was incorporated into the analysis using diffuser analogy. A cascade-based correlation for maximum static pressure-rise coefficient as a function of area ratio, divergence angle, and turning provides the basis for estimation. Comparison with several experimentally demonstrated values confirmed the adequacy of the prediction as a qualitative measure of stall margin capability.

3. The cascade-based pressure-loss coefficient model was replaced by a model that had been developed and validated using compressor test results. The new model, which accounts for several dependencies not found in the previous model, includes profile loss, endwall loss, and shock loss correlations. Efficiencies calculated for five compressors and one fan all matched experimentally-based values to within one point.

4. Default correlations for rotor and stator solidities and aspect ratios and for stator-exit tangential velocity along with default values for the aerodynamic design limits have been added to the code as an aid to non-expert users in selecting reasonable values for these inputs. Rotor-tip solidity is a function of rotor-tip inlet Mach number and stator-hub solidity

depends on stator hub flow turning. Aspect ratio depends on stage location. The stator-exit tangential velocities are based on a mid-stage reaction along with an assumed stagewise distribution. Aerodynamic design limits for rotor and stator diffusions, rotor hub turning, and stator-hub Mach number are based on experience.

This report is also an updated users manual for the modified CSPAN code. Program input and output are described, and sample cases are included for illustration.

REFERENCES

1. Bryans, A.C.; and Miller, M.L.: Computer Program for Design of Multistage Axial-Flow Compressors. NASA CR-54530, 1967.

2. Glassman, A.J.: Users Manual for Updated Code for Axial-Flow Compressor Conceptual Design. NASA CR-189171, 1992.

3. Glassman, A.J.: Blading Models for TURBAN and CSPAN Turbomachine Codes. NASA CR-191164, 1993.

4. Wright, P.I.; and Miller, D.C.: An Improved Compressor Performance Prediction Model. IMechE, C423/028, 1991.

5. Schweitzer, J.K.; and Garberoglio, J.E.: Maximum Loading Capability of Axial Flow Compressors. J. Aircraft, vol. 21, no. 8, Aug. 1984, pp. 593-600.

6. De Ruyck, J.; and Hirsch, C.: Investigations of an Axial Compressor End-Wall Boundary Layer Prediction Method. ASME Paper 80-GT-53, 1980.

7. Glassman, A.J.: Basic Turbine Concepts. Ch. 2 of Turbine Design and Application, vol. 1, A.J. Glassman, ed., NASA SP-290, 1972, pp. 21-67.

TABLE I. -
COMPARISON OF COMPUTED AND EXPERIMENTAL PERFORMANCE

Number of stages	Total pressure ratio	Computed efficiency	Experimental efficiency	Computed stall margin	Experimental stall margin
10	23.0	0.848	0.855	22.9	16.4
10	14.0	.865	.862	17.7	16.7
8	10.3	.884	.875	14.9	14.3
5	5.0	.868	.867	27.1	----
3	4.5	.851	.860	20.4	16.3
1	1.65	.894	.886	13.5	15.

TABLE II. - SAMPLE INPUT

```
    5 STAGE TRANSONIC COMPRESSOR WITH DEFAULT INPUT
&NAME TTI=518.7,PTI=14.7,RCLIM=5.0,RTIP1I=10.,
UTIP1I=1100.,RHORT1=.5,VZTIPO=-67.5,NPRI=5*-1.,N=3,NSLIM=5,NPSI=5*-1.,
&END
    NACA 5 STAGE TRANSONIC COMPRESSOR
&NAME MW=29.,GAM=1.4,TTI=518.7,PTI=14.7,RCLIM=5.0,RTIP1I=10.,
UTIP1I=1100.,RHORT1=.5,VZTIPO=-67.5,NPRI=5*-1.,N=3,NSLIM=5,
RT2OT1=5*1.0,SRTIP=0.98,1.17,1.30,1.14,0.99,B1=0.0,
VT2OT1=.918,.885,.916,.909,.916,
ARHD=5*40.,ARTD=5*-20.,ARO=2.,1.52,1.11,0.99,0.92,DRT=5*.45,
ASHD=5*40.,ASTD=5*-20.,VT3OT2=1.094,1.071,1.053,1.057,0.992,NPSI=5*-1.,
SSH=1.8,1.9,1.6,1.5,1.4,ASO=2.15,1.63,1.24,1.01,0.88,
DSH=5*.55,MSH=5*.75,BPSD=5*45.,B3=5*0.0,RT3OT2=5*1.0,
&END
```

TABLE III. - CONVERGENCE OUTPUT FOR SAMPLE CASE

```
CPR=  5.000000000     NOT ACHIEVED IN          5 STAGES: CPR=  4.738175869


STAGES=           5
DRTK=  1.000000000     CPR=  5.550810337     EFF= 0.8655098081
DRTK= 0.9007693529     CPR=  4.878148556     EFF= 0.8671319485
DRTK= 0.9187448025     CPR=  4.999482155     EFF= 0.8674436212
DRTK= 0.9188215137     CPR=  5.000028610     EFF= 0.8674529195
STALL MARGIN=  27.04190826
```

TABLE IV.—MAIN OUTPUT FOR SAMPLE CASE

NACA 5 STAGE TRANSONIC COMPRESSOR

LOSS MODEL: INTERNAL CORRELATION FOR TOTAL-PRESSURE LOSS COEFFICIENTS

*** I N L E T I N P U T D A T A ***

NO. RAD. STATIONS	NUMBER STAGES	SP. HEAT (BTU/(LB-R))	MOL. WT. (MOLES)	RATIO OF SP. HEAT	IN. TOT. TEMP. (DEG. R)	IN. TOT. PR. (PSI)	MASS AVG. TOT. PR. RATIO	IGV DEL P/P
3	5	.2400	28.9700	1.4000	518.7000	14.7000	5.0000	.000

*** R O T O R I N L E T I N P U T D A T A ***

TIP RADIUS (INCHES)	TIP WHEEL SPEED (FT/SEC)	HUB TO TIP RADIUS RATIO	MASS FLOW (LB/SEC)	TIP BLOCKAGE FACTOR	HUB BLOCKAGE FACTOR	ROT. SPEED (RPM)
10.0000	1100.0000	.5000	67.5000	.9900	.9900	12605.08

COEFFICIENTS IN TANGENTIAL VELOCITY EQUATION

B	C	D	E
.0000	.0000	.0000	.0000

****

*** STATOR HUB MACH NO. LIMIT VIOLATED ***

TABLE IV.—Continued.

******** S T A G E D A T A ********

STAGE NO. 1

*** ROTOR INPUT DATA ***

MERID VEL. RATIO	POLYTROPIC EFFICIENCY	SOLIDITY AT TIP	ASPECT RATIO	TIP BLOCKAGE FACTOR	HUB BLOCKAGE FACTOR	MAX ANGLE HUB TAPER (DEGREES)	MAX ANGLE TIP TAPER (DEGREES)
.9180	.9226	.9800	2.0000	.9903	.9953	40.000	-20.000

MAX ROTOR DIF. FACTOR	MAX. TURNING ANGLE ROTOR HUB (DEGREES)	TIP RADIUS RATIO	COEFFICIENTS IN TANGENTIAL VELOCITY EQUATION B	C	D	E
.4135	45.0000	1.000	.0000	.0000	.0000	.0000

*** STATOR INPUT DATA ***

MERID VELOCITY RATIO	STAGE POLYTROPIC EFFICIENCY	SOLIDITY AT HUB	ASPECT RATIO	TIP BLOCKAGE FACTOR	HUB BLOCKAGE FACTOR	MAX ANGLE HUB TAPER (DEGREES)	MAX ANGLE TIP TAPER (DEGREES)
1.0940	.8954	1.8000	2.1500	.9769	.9879	40.0000	-20.0000

MAX. STATOR DIF. FACTOR	MAX HUB INLET MACH NUMBER	TIP RADIUS RATIO	COEFFICIENTS IN TANGENTIAL VELOCITY EQUATION B	C	D	E
.5500	.7500	1.000	.0000	.0000	.0000	.0000

—**— S T A G E O U T P U T D A T A ***—**—***

MASS FLOW (LB/SEC) = 67.500

OVERALL MASS AVE. PR. RATIO	OVERALL MASS AVE. TEMP. RATIO	OVERALL MASS AVE. EFFICIENCY	MASS AVE. PRESSURE RATIO	MASS AVE. TEMPERATURE RATIO	MASS AVE. EFFICIENCY	ROTOR ASPECT RATIO	STATOR ASPECT RATIO	OVERALL MASS AVE. POLY EFF.
1.4273	1.1202	.8900	1.4273	1.1202	.8900	2.0000	2.1500	.8954

ROTOR TIP RAD. 1-G (INCHES)	ROTOR HUB RAD. 1-G (INCHES)	ROTOR TIP RAD. 2-G (INCHES)	ROTOR HUB RAD. 2-G (INCHES)	STATOR TIP RAD. 3-G (INCHES)	STATOR HUB RAD. 3-G (INCHES)	ROTOR PROJ. LENGTH (INCHES)	STATOR PROJ. LENGTH (INCHES)
10.0000	5.0000	10.0000	5.8172	10.0000	6.3848	2.3685	1.9058

ROTOR TIP RAMP ANGLE (DEGREES)	ROTOR HUB RAMP ANGLE (DEGREES)	STATOR TIP RAMP ANGLE (DEGREES)	STATOR HUB RAMP ANGLE (DEGREES)
.0000	19.0363	.0000	16.5857

—**— R O T O R I N L E T O U T P U T D A T A ***—**—***

STA NO.	RADIUS -E (IN)	WHEEL SPEED (FT/SEC)	MERID VEL. (FT/SEC)	TANGENT. VEL. (FT/SEC)	ABS. VEL. (FT/SEC)	REL. VEL. (FT/SEC)	ABS. AIR ANG. (DEG)	REL. AIR ANG. (DEG)	TOTAL TEMP. (DEG R)	TOTAL PRESS. (PSI)	REL. MACH NO.	ABS. MACH NO.	SHOCK LOSS COEFF	TOTAL LOSS COEFF	ROTOR DIF. FACTOR
1	9.962	1095.867	659.252	.000	659.252	1278.882	.000	58.970	518.700	14.700	1.188	.612	.017	.067	.379
2	7.518	827.028	659.252	.000	659.252	1057.634	.000	51.440	518.700	14.700	.982	.612	.017	.067	.438
3	5.074	558.189	659.252	.000	659.252	863.822	.000	40.255	518.700	14.700	.802	.612	.017	.067	.457

—**— R O T O R E X I T O U T P U T D A T A ***—**—***

STA NO.	RADIUS -E (IN)	WHEEL SPEED (FT/SEC)	MERID VEL. (FT/SEC)	TANGENT. VEL. (FT/SEC)	ABS. VEL. (FT/SEC)	REL. VEL. (FT/SEC)	ABS. AIR ANG. (DEG)	REL. AIR ANG. (DEG)	TOTAL TEMP. (DEG R)	TOTAL PRESS. (PSI)	SPANL INCL (DEG)	REL. MACH NO.	ABS. MACH NO.	STAGE REACTION
1	9.968	1096.451	605.193	341.651	694.971	967.461	29.446	51.278	581.060	21.025	.000	.849	.610	.935
2	7.906	869.635	605.193	430.760	742.841	747.577	35.442	35.949	581.060	21.228	9.133	.659	.655	.844
3	5.844	642.819	605.193	582.751	840.154	608.167	43.918	5.668	581.060	21.398	17.824	.543	.750	.638

—**— S T A T O R E X I T O U T P U T D A T A ***—**—***

STA NO.	RADIUS -E (IN)	MERID VEL. (FT/SEC)	TANGENT. VEL. (FT/SEC)	ABS. VEL. (FT/SEC)	SPANL. INCL. (DEG)	ABS. AIR ANG. (DEG)	TOTAL PRESS (PSI)	SHOCK LOSS COEFF	TOTAL LOSS COEFF	STATOR DIF. FACTOR	MERID MACH NO.	ABS. MACH NO.
1	9.931	662.081	.000	662.081	.000	.000	20.829	.000	.042	.269	.579	.579
2	8.186	662.081	.000	662.081	8.115	.000	21.005	.000	.042	.320	.579	.579
3	6.441	662.081	.000	662.081	15.917	.000	21.118	.000	.042	.405	.579	.579

—**— B L A D I N G G E O M E T R Y O U T P U T ***—**—***

ROTOR — NO. OF BLADES= 25. CHORD LENGTH = 2.50 IN.

	AXIAL CHORD	ACTUAL SOLID	STAG. ANGLE	INCID ANGLE	DEVIA ANGLE	CAMBER ANGLE	BLD IN ANGLE	BLD EX ANGLE
1	1.466	.983	54.09	.33	1.75	9.11	58.64	49.53
2	1.881	1.271	40.79	-.53	6.33	22.36	51.97	29.62
3	2.369	1.795	17.66	.78	9.82	43.63	39.47	-4.16

STATOR — NO. OF VANES= 35. CHORD LENGTH = 1.95 IN.

	AXIAL CHORD	ACTUAL SOLID	STAG. ANGLE	INCID ANGLE	DEVIA ANGLE	CAMBER ANGLE	BLD IN ANGLE	BLD EX ANGLE
1	1.906	1.104	11.60	-1.98	8.24	39.67	31.43	-8.24
2	1.889	1.365	13.73	-1.52	9.51	46.48	36.97	-9.51
3	1.863	1.788	16.11	-.25	11.95	56.11	44.16	-11.95

TABLE IV.—Concluded.

******** S T A G E D A T A ********

STAGE NO. 5

*** ROTOR INPUT DATA ***

MERID VEL. RATIO	POLYTROPIC EFFICIENCY	SOLIDITY AT TIP	ASPECT RATIO	TIP BLOCKAGE FACTOR	HUB BLOCKAGE FACTOR	MAX ANGLE HUB TAPER (DEGREES)	MAX ANGLE TIP TAPER (DEGREES)
.9160	.9139	.9900	.9200	.9824	.9881	40.000	-20.000

MAX ROTOR DIF. FACTOR	MAX. TURNING ANGLE ROTOR HUB (DEGREES)	TIP RADIUS RATIO	COEFFICIENTS IN TANGENTIAL VELOCITY EQUATION B	C	D	E
.4135	45.0000	1.000	.0000	.0000	.0000	.0000

*** STATOR INPUT DATA ***

MERID VELOCITY RATIO	STAGE POLYTROPIC EFFICIENCY	SOLIDITY AT HUB	ASPECT RATIO	TIP BLOCKAGE FACTOR	HUB BLOCKAGE FACTOR	MAX ANGLE HUB TAPER (DEGREES)	MAX ANGLE TIP TAPER (DEGREES)
.9920	.8868	1.4000	.8800	.9393	.9572	40.0000	-20.0000

MAX. STATOR DIF. FACTOR	MAX HUB INLET MACH NUMBER	TIP RADIUS RATIO	COEFFICIENTS IN TANGENTIAL VELOCITY EQUATION B	C	D	E
.5500	.7500	1.000	.0000	.0000	.0000	.0000

—**— S T A G E O U T P U T D A T A ***—**—***

MASS FLOW (LB/SEC) = 67.500

OVERALL MASS AVE. PR. RATIO	OVERALL MASS AVE. TEMP. RATIO	OVERALL MASS AVE. EFFICIENCY	MASS AVE. PRESSURE RATIO	MASS AVE. TEMPERATURE RATIO	MASS AVE. EFFICIENCY	ROTOR ASPECT RATIO	STATOR ASPECT RATIO	OVERALL MASS AVE. POLY EFF.
5.0000	1.6730	.8675	1.2841	1.0839	.8827	.9200	.8800	.8935

ROTOR TIP RAD. 1-G (INCHES)	ROTOR HUB RAD. 1-G (INCHES)	ROTOR TIP RAD. 2-G (INCHES)	ROTOR HUB RAD. 2-G (INCHES)	STATOR TIP RAD. 3-G (INCHES)	STATOR HUB RAD. 3-G (INCHES)	ROTOR PROJ. LENGTH (INCHES)	STATOR PROJ. LENGTH (INCHES)
10.0000	8.1952	10.0000	8.4270	10.0000	8.3324	1.3440	1.7361

ROTOR TIP RAMP ANGLE (DEGREES)	ROTOR HUB RAMP ANGLE (DEGREES)	STATOR TIP RAMP ANGLE (DEGREES)	STATOR HUB RAMP ANGLE (DEGREES)
.0000	9.7865	.0000	-3.1196

—**— R O T O R I N L E T O U T P U T D A T A ***—**—***

STA NO.	RADIUS -E (IN)	WHEEL SPEED (FT/SEC)	MERID VEL. (FT/SEC)	TANGENT. VEL. (FT/SEC)	ABS. VEL. (FT/SEC)	REL. VEL. (FT/SEC)	ABS. AIR ANG. (DEG)	REL. AIR ANG. (DEG)	TOTAL TEMP. (DEG R)	TOTAL PRESS. (PSI)	REL. MACH NO.	ABS. MACH NO.	SHOCK LOSS COEFF	TOTAL LOSS COEFF	ROTOR DIF. FACTOR
1	9.921	1091.349	581.577	.000	581.577	1236.638	.000	61.947	800.621	56.114	.908	.427	.000	.064	.417
2	9.091	1000.018	581.576	.000	581.576	1156.835	.000	59.819	800.621	57.330	.849	.427	.000	.064	.451
3	8.261	908.686	581.576	.000	581.576	1078.861	.000	57.380	800.621	58.247	.792	.427	.000	.064	.488

—**— R O T O R E X I T O U T P U T D A T A ***—**—***

STA NO.	RADIUS -E (IN)	WHEEL SPEED (FT/SEC)	MERID VEL. (FT/SEC)	TANGENT. VEL. (FT/SEC)	ABS. VEL. (FT/SEC)	REL. VEL. (FT/SEC)	ABS. AIR ANG. (DEG)	REL. AIR ANG. (DEG)	TOTAL TEMP. (DEG R)	TOTAL PRESS. (PSI)	SPANL INCL (DEG)	REL. MACH NO.	ABS. MACH NO.	STAGE REACTION
1	9.974	1097.183	532.724	367.810	647.363	903.205	34.622	53.856	867.801	72.426	.000	.638	.458	.900
2	9.211	1013.204	532.725	398.296	665.158	813.577	36.784	49.096	867.801	74.188	1.681	.576	.471	.871
3	8.448	929.225	532.725	434.292	687.318	727.155	39.188	42.894	867.801	75.565	3.360	.515	.487	.834

—**— S T A T O R E X I T O U T P U T D A T A ***—**—***

STA NO.	RADIUS -E (IN)	MERID VEL. (FT/SEC)	TANGENT. VEL. (FT/SEC)	ABS. VEL. (FT/SEC)	SPANL. INCL. (DEG)	ABS. AIR ANG. (DEG)	TOTAL PRESS (PSI)	SHOCK LOSS COEFF	TOTAL LOSS COEFF	STATOR DIF. FACTOR	MERID MACH NO.	ABS. MACH NO.
1	9.907	528.462	.000	528.462	.000	.000	71.903	.000	.054	.423	.371	.371
2	9.159	528.463	.000	528.463	-1.561	.000	73.625	.000	.054	.439	.371	.371
3	8.411	528.463	.000	528.463	-3.120	.000	74.954	.000	.054	.457	.371	.371

—**— B L A D I N G G E O M E T R Y O U T P U T ***—**—***

ROTOR — NO. OF BLADES= 32. CHORD LENGTH = 1.96 IN.

	AXIAL CHORD	ACTUAL SOLID	STAG. ANGLE	INCID ANGLE	DEVIA ANGLE	CAMBER ANGLE	BLD IN ANGLE	BLD EX ANGLE
1	1.075	.995	56.76	-.05	2.34	10.49	62.00	51.52
2	1.199	1.082	52.21	-1.22	5.72	17.66	61.04	43.38
3	1.344	1.185	46.34	-2.24	9.84	26.57	59.62	33.05

STALL MARGIN= 27.0

STATOR — NO. OF VANES= 41. CHORD LENGTH = 1.79 IN.

	AXIAL CHORD	ACTUAL SOLID	STAG. ANGLE	INCID ANGLE	DEVIA ANGLE	CAMBER ANGLE	BLD IN ANGLE	BLD EX ANGLE
1	1.736	1.180	13.76	-2.61	9.72	46.96	37.24	-9.72
2	1.733	1.277	14.15	-2.51	11.00	50.29	39.30	-11.00
3	1.733	1.392	14.21	-2.39	13.15	54.72	41.58	-13.15

*** OVERALL PRESSURE RATIO LIMIT HAS BEEN REACHED — GO TO NEW DATA ***

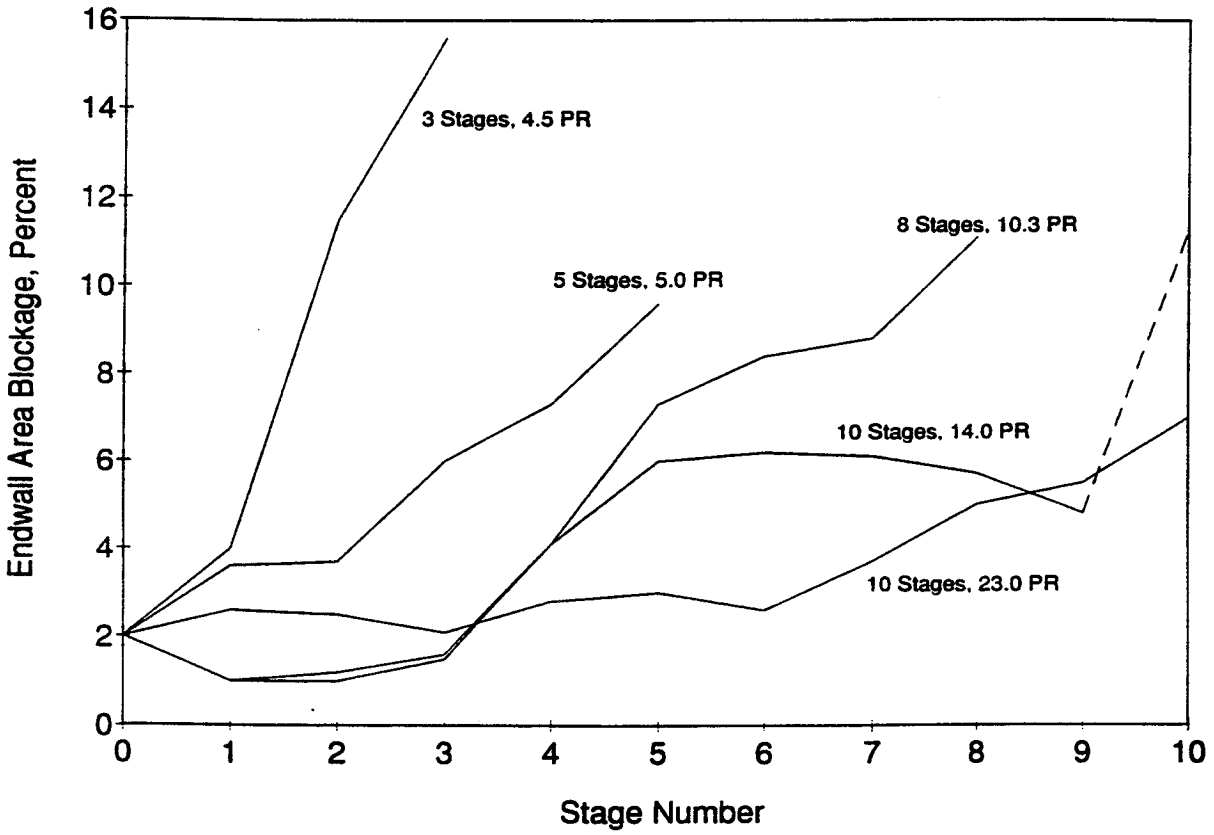

Figure 1.--Stage-exit endwall-area blockage calculation results

REPORT DOCUMENTATION PAGE

Form Approved
OMB No. 0704-0188

1. AGENCY USE ONLY (*Leave blank*)	2. REPORT DATE	3. REPORT TYPE AND DATES COVERED
	January 1995	Technical Memorandum

4. TITLE AND SUBTITLE

Enhanced Capabilities and Modified Users Manual for Axial-Flow Compressor Conceptual Design Code CSPAN

5. FUNDING NUMBERS

WU–505–69–50

6. AUTHOR(S)

Arthur J. Glassman and Thomas M. Lavelle

7. PERFORMING ORGANIZATION NAME(S) AND ADDRESS(ES)

National Aeronautics and Space Administration
Lewis Research Center
Cleveland, Ohio 44135–3191

8. PERFORMING ORGANIZATION REPORT NUMBER

E–9394

9. SPONSORING/MONITORING AGENCY NAME(S) AND ADDRESS(ES)

National Aeronautics and Space Administration
Washington, D.C. 20546–0001

10. SPONSORING/MONITORING AGENCY REPORT NUMBER

NASA TM–106833

11. SUPPLEMENTARY NOTES

Arthur J. Glassman, University of Toledo, Toledo, Ohio 43606 and Resident Research Associate at NASA Lewis Research Center; Thomas M. Lavelle, NASA Lewis Research Center. Responsible person, Thomas M. Lavelle, organization code 2410, (216) 433–7042.

12a. DISTRIBUTION/AVAILABILITY STATEMENT

Unclassified - Unlimited
Subject Category 02

This publication is available from the NASA Center for Aerospace Information, (301) 621–0390.

12b. DISTRIBUTION CODE

13. ABSTRACT (*Maximum 200 words*)

Modifications made to the axial-flow compressor conceptual design code CSPAN are documented in this report. Endwall blockage and stall margin predictions were added. The loss-coefficient model was upgraded. Default correlations for rotor and stator solidity and aspect-ratio inputs and for stator-exit tangential velocity inputs were included in the code along with defaults for aerodynamic design limits. A complete description of input and output along with sample cases are included.

14. SUBJECT TERMS

Axial-flow compressor; Compressor analysis

15. NUMBER OF PAGES

24

16. PRICE CODE

A03

17. SECURITY CLASSIFICATION OF REPORT	18. SECURITY CLASSIFICATION OF THIS PAGE	19. SECURITY CLASSIFICATION OF ABSTRACT	20. LIMITATION OF ABSTRACT
Unclassified	Unclassified	Unclassified	